



OMV AUSTRALIA PTY LTD

ACN 082 932 027

SOLE DEVELOPMENT

(Patricia Baleen Extension)

Geology

SD-01-RE-0012

Part D

March 2004

Table of Contents

1	INTRODUCTION	2
2	Reservoir Geology	3
2.1	Depositional Model	3
2.2	Well Log Correlation and Facies Coding	5
3	Structural Modelling	7
3.1	Fault Modelling	7
3.2	Stratigraphic Modelling	7
3.3	3D Gridding	7
4	Data Analysis	8
4.1	Relationship Between Facies and Petrophysical Parameters	8
4.2	Facies Split in the Stratigraphic Units	9
4.3	Investigation of Possible Trends in the Data	9
5	Property Modelling	10
5.1	Facies	10
5.1.1	Base Case	10
5.1.2	Conservative Scenario	10
5.2	Porosity and Permeability	11
5.3	Water Saturation	12
6	Volumetrics (GIP)	14
6.1	Base Case GIP	14
6.2	GIP Effect of 8% shales Between the Wells	14
6.3	GIP Effect of Optimistic Seismic Pick	15
6.4	GIP Effect of Conservative Seismic Pick	15
6.5	Summary of GIP Volumetrics from 3D modelling	16
7	Simulation Grid Design	18
8	Upscaling and Grid Export for Simulation	19

Figures

Figure D1	Top Latrobe Depth Map	2
Figure D2	Outcrop Analog of Latrobe Sheetflood Deposits	4
Figure D3	Sole Field Modern Reservoir Analog	5
Figure D4	Dart-1, Sole-1 and Sole-2 Correlation Panel	6
Figure D5	Porosity Distribution by Facies	8
Figure D6	Permeability Distribution by Facies	8
Figure D7	Permeability (in Darcies) vs Depth in the Braided Channels Facies	9
Figure D8	Model with 8% volume shale and all other facies filtered out	11
Figure D9	Petrophysical Conditioning	12
Figure D10	Height above Free Water Level used in the Water Saturation Calculations	13
Figure D11	GIP in modelled scenarios	17
Figure D12	Illustration of the Upscaling Process of Porosity	19

Tables

Table D1	Base Case GIP	14
Table D2	GIP Effect of 8% Shales Between the Wells.....	15
Table D3	GIP Effect of Optimistic Seismic Pick	15
Table D4	GIP Effect of Conservative Seismic Pick	16
Table D5	Comparison Simulation Model vs Geological Model Volumetrics.....	20

Enclosures

Enclosure D1 Correlation Panel and Facies Coding

SUMMARY

A 3D geologic modelling study of the Sole Field has been carried out to achieve a better understanding of the Sole Field and to quantify the uncertainties in the volumes and fluid flow. 3D models with different reasonable geological scenarios have been generated, and the resulting volumetric range has been calculated. Representative models for each of the scenarios have then been used to create simulation grids with upscaled properties. These upscaled models have been exported to Eclipse for dynamic reservoir modelling.

Four different scenarios of the Sole field have been investigated, namely:

- Base case (the most likely structure and the facies volume fraction from the wells)
- 8% shale between the wells (the most likely structure, but added 8 % non-net shale to the model. This shale is not observed in the reservoir units in the two wells)
- Optimistic seismic pick (the upside structure and the facies volume fraction from the wells)
- Conservative seismic pick (the downside structure and the facies volume fraction from the wells)

For each of these cases, ten realizations of facies and petrophysics have been generated and GIP has been calculated. The result of the study shows that the range in volumes remains relatively tight. The GIP mean values for the modelled scenarios are as follows:

- | | |
|------------------------------|--|
| • Base case | 358.7 BCF (P50 = 358.5 BCF) |
| • 8% shale between the wells | 327.2 BCF (8.8% lower than P50 base case) |
| • Optimistic seismic pick | 379.5 BCF (5.8% higher than P50 base case) |
| • Conservative seismic pick | 352.1 BCF (1.8% lower than P50 base case) |

The additional uncertainty related to parameter distribution (reservoir facies, porosity and water saturation) in each of these scenarios is small (approx +3 %).

The P50 models were exported to Eclipse for flow simulation.

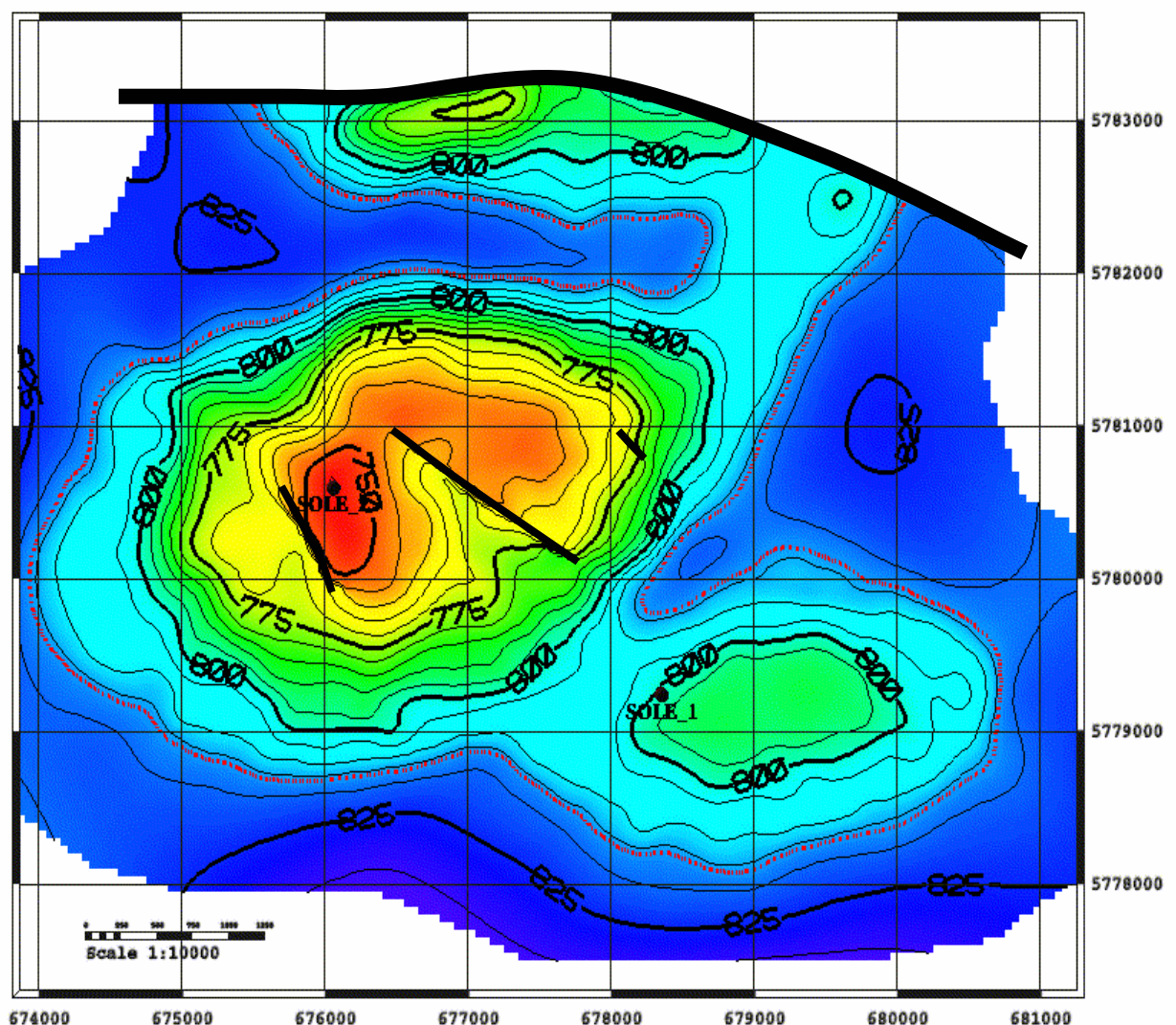
1 INTRODUCTION

The Sole gas field is located in Retention License VIC/RL3 in the offshore Gippsland Basin, Victoria. The Sole-1 discovery well drilled in 1973 by Shell Development Australia, is located in an off-crest position on the southeast flank of the Sole field.

The Sole-2 appraisal well was drilled at the crest of the Sole anticline in July 2002 and was located on a regular 1 x 1 km 2D seismic grid that had been reprocessed that year. This well proved the presence of a significant gas resource, with the well intersecting a 70+m gas column in high quality sandstones at the top of the Latrobe Group. The field is constrained to the north by a major E-W fault.

This report describes the results of the 3D geological modelling of the Sole field. The modelling is based on data from both Sole-1 and Sole-2 and a depth map of the Top Latrobe Group (Figure D1). The map is based on interpretation of a 2D seismic grid with line spacing 500*250 m. Most of the seismic grid was recorded in 2003.

Figure D1 **Top Latrobe Depth Map**



Only three faults have been interpreted within the gas reservoir. These are shown as the three thick black lines in the centre of map (The two biggest faults are on either side of Sole-2, with strike SE-NW). The northern boundary of the field is a major E-W fault along the northern limit of the map.

2 RESERVOIR GEOLOGY

2.1 Depositional Model

Sole Gas Field is trapped within the top Latrobe Group coarse clastics in a gentle simple anticline on an east-west structural terrace between the main depocentre and the basin edge. This structure formed during the Late Eocene transpressional event that created many of the Gippsland Basin hydrocarbon-bearing structures. The gas pool is bounded along its northern margin by an east-west reverse fault, which fades towards the basin, being normal to the east and west of Sole but increasingly inverted across the field where the throw becomes reversed. Other than three small scale crestal faults, the reservoir is unfaulted on the 2D seismic data set.

This part of the basin is characterised by a relatively thin Latrobe Group sequence, unconformably deposited over Emperor Subgroup or Strzelecki Group sediments and basement (north of the field bounding fault). The Latrobe Group which contains the main reservoirs in the basin, was deposited as a non-marine to marginal marine clastic sequence from the Late Campanian to Late Eocene. Regionally, the top of the Latrobe Group is marked by a gradual marine transgression which ultimately led to the deposition of the overlying shelfal and deep marine sediments of the Gurnard, Lakes Entrance and Gippsland Limestone Formations.

The Gurnard is a transitional glauconitic sandstone unit that is absent in the Sole wells. The unit is usually a waste zone or seal but forms the gas reservoir in the Patricia-Baleen fields along strike to the west. The Lakes Entrance Formation forms the seal for the Sole field.

Detailed stratigraphic subdivision of the Latrobe Group is based on good seismic control and palynological zonation of samples from a number of wells.

Along the Sole fault terrace, the upper Latrobe consists of non-marine sands that possess good reservoir qualities. Increased depositional energies in the upper part of the Latrobe are commonly expressed by an upwards decrease of carbonaceous sediments in favour of sandstones with high net to gross reservoir.

At Sole, the Latrobe Group is 200m thick and comprises two depositional cycles, namely a lower high energy coastal plain sequence overlain by a thin section of argillaceous sandstone with marine influences (Kate Shale equivalent), followed by a second cycle with higher energy non-marine coastal plain sediments. The gas reservoir occurs in the younger cycle in this package. Depositional environments in the reservoir have been calibrated to the sedimentological features observed in the four conventional cores recovered from Sole-2 and the interpretation of FMI images from that well. There was no conventional coring in Sole-1. Dipmeter tadpoles¹ from the discovery well have been digitised and are shown on Enclosure D1 although there is low confidence in them.

The integrated interpretation of these data from Sole-2 is consistent with the reservoir being comprised of alternating cycles of sheetflood and fluvial channel deposits. The same lithofacies are developed in Sole-1, 2.75km to the southeast.

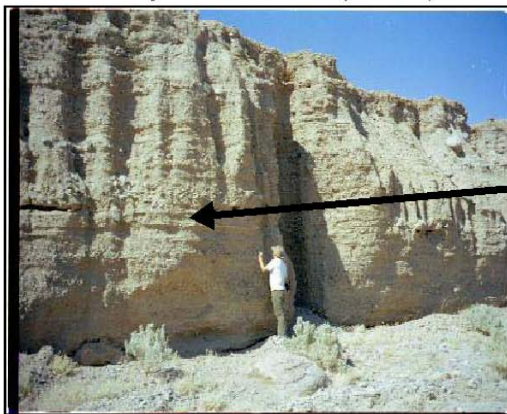
¹ The original Sole-1 digital dipmeter data from the well is no longer available

Sole-2 structural dip is 5° to an azimuth of 095° , similar to the structural dip of the Kate Shale equivalent. The reservoir interval in the well is dominated by low angle sheet flood deposits with depositional dip values ranging from 3° - 11° , typical of outwash fan deposits. The orientation of the reservoir has been established to be a fan shaped deposit transported from a major source in the west. A secondary sediment source may also have existed north of the main bounding fault where seismic data suggests the presence of an uplifted basement block during Latrobe Group deposition. Major channel scour and depositional episodes show very strong west to east planar cross bedding (current) dips. The fluvial component from 789-798m is a strong unimodal (west to east) channel scoured into the underlying sheet flood deposit and running roughly parallel with the orientation of the Sole terrace and the northern bounding fault.

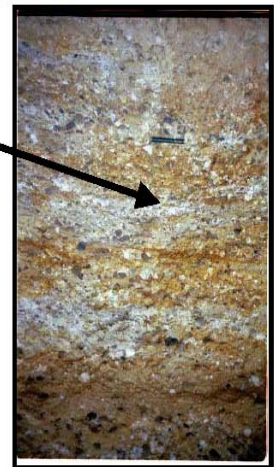
Figure D2 shows a field outcrop analog of sheetflood sands, similar to those in the Sole reservoir, while Figure D3 shows a modern example with both radial fan sediments and axial fluvial deposits being transported to a downstream standing body of water. Lagoonal or lacustrine deposits would be expected east of the Sole field in lower energy, lower coastal plain environments closer to the Paleocene shoreline in the eastern part of the basin. Such a setting is consistent with the deposits and palynofacies recognised in Sole-1.

Figure D2 Outcrop Analog of Latrobe Sheetflood Deposits

Death Valley sheet flood deposits (author)



Possible sheet flood deposit in high energy continental setting – implies lack of organised bedding to weak planar bedding as seen in the outcrop image to the left.

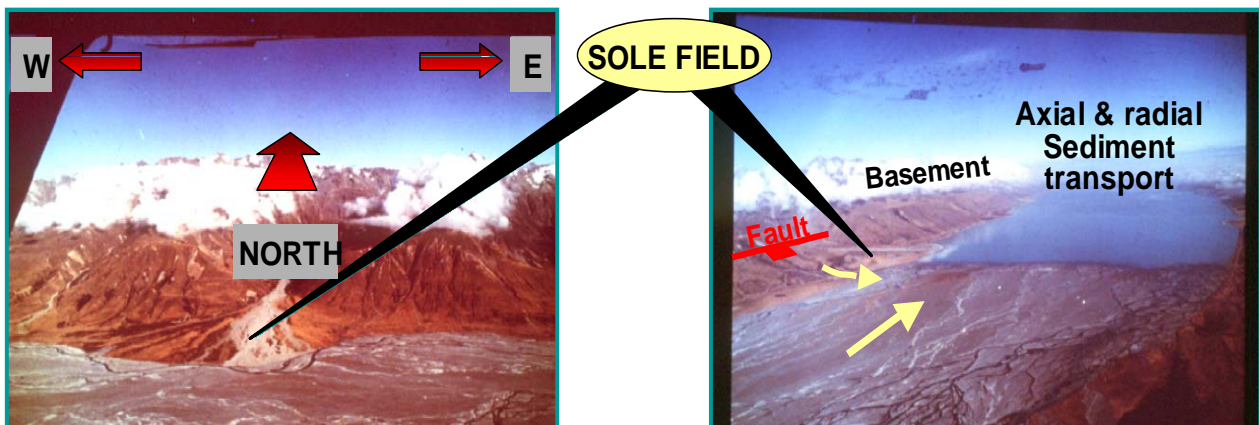


Note:

Sole – 2 reservoir section contains very well developed planar bedding

Distributed in a 200 degree azimuthal range –indicating sheet and debris flows for much of the section interrupted by channel deposits flowing west – east.

Figure D3

Sole Field Modern Reservoir Analog

The sole – 2 sediments exhibit a high degree of organisation and planar bedding indicating substantial periods of shallow water entrainment and sediment distribution in numerous sheet flood deposits mixed with fluvial channel cycles. The proximity to clay islands or banks is a given from the presence of shale clasts. The clean nature of the sediment also suggests entrainment, and the pebbly nature of the section indicates proximity to clastic source. Paucity of carbonaceous suggests that the area was not heavily vegetated at this location.

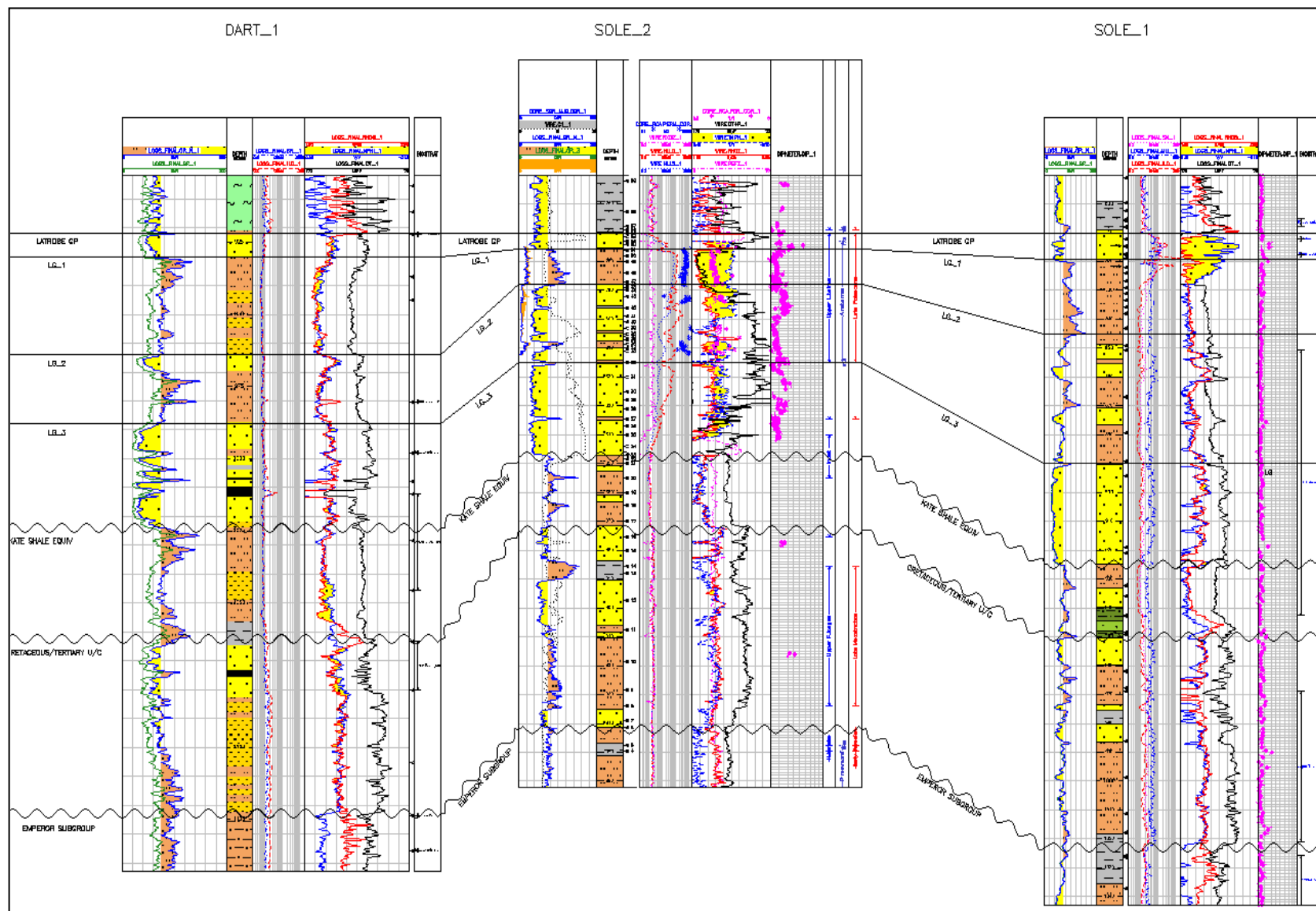
2.2 Well Log Correlation and Facies Coding

Based on core and the logs from Sole-1 and Sole-2, the reservoir has been interpreted to consist of two facies types: Braided Channels and Sheetflood. The same facies also extend to Dart-1, outside the field area, 8 km southwest of Sole-2. Recognition of these facies is based on the sedimentology of cores in Sole-2 and its calibration to the FMI log. No other facies are observed in these two wells in the layers of interest. The reservoir has been subdivided into 5 stratigraphic layers:

- Latrobe GP (Top Latrobe interpreted on seismic)
- LG_1
- LG_2
- LG_3
- Kate Shale Eqiv. The top 20 meters of this layer is included in the modelling.

A correlation panel is displayed in Figure D4 (a larger version is attached as Enclosure D1).

Figure D4 *Dart-1, Sole-1 and Sole-2 Correlation Panel*



Facies coding (depth track) : Yellow = Braided channels, Brown = Sheetflood. Grey = Claystone/Shale (See also Enclosure D1).

3 STRUCTURAL MODELLING

3.1 Fault Modelling

Only three faults within the reservoir have been interpreted from the 2D seismic data set and have been included in the model (See Figure D1).

3.2 Stratigraphic Modelling

Stratigraphic modelling was performed from top to bottom using the well picks from the correlation panel (Figure D2 / Enclosure D1). This resulted in the calculated horizons LG1, LG2, LG3 and Kate Shale Equivalent. The base of the Kate Shale Equivalent unit was set to 20 meters below the top.

3.3 3D Gridding

A 3D grid with 5 subgrids (one for each stratigraphic layer) was then generated. The facies log was investigated first to broadly assess the heterogenities (in order to determine the vertical resolution). Heterogenities are more pronounced in LG_2 than in the other stratigraphic units. (Figure D2 / Enclosure D1). A vertical resolution of approximately 1 meter has been selected as sufficient for modelling purposes.

The following resolution was used to generate the 3D geological modelling grid:

- XY resolution: 100*100m
- Z(vertical) resolution: a constant number of layers that resulted in an approximate thickness of 1 meter in every subgrid:

• Subgrid 1 (Latrobe GP)	6 layers
• Subgrid 2 (LG_1)	12 layers
• Subgrid 3 (LG_2)	25 layers
• Subgrid 4 (LG_3)	30 layers
• Subgrid 5 (Top 20 m of Kate Shale Eqiv)	20 layers

4 DATA ANALYSIS

4.1 Relationship Between Facies and Petrophysical Parameters

In Sole-1 and Sole-2, the logs of permeability (PERM) and porosity (PHIT) were generated as described in Part B. These logs were imported into RMS, and every upscaled log sample within the layers of interest were used to generate histograms of Porosity (PHIT) and Permeability (PERM) colour coded by facies (Red = Braided Channels, Blue = Sheetflood). This was carried out in order to investigate relationships between these petrophysical properties and the facies coding in the wells Sole-1 and Sole-2:

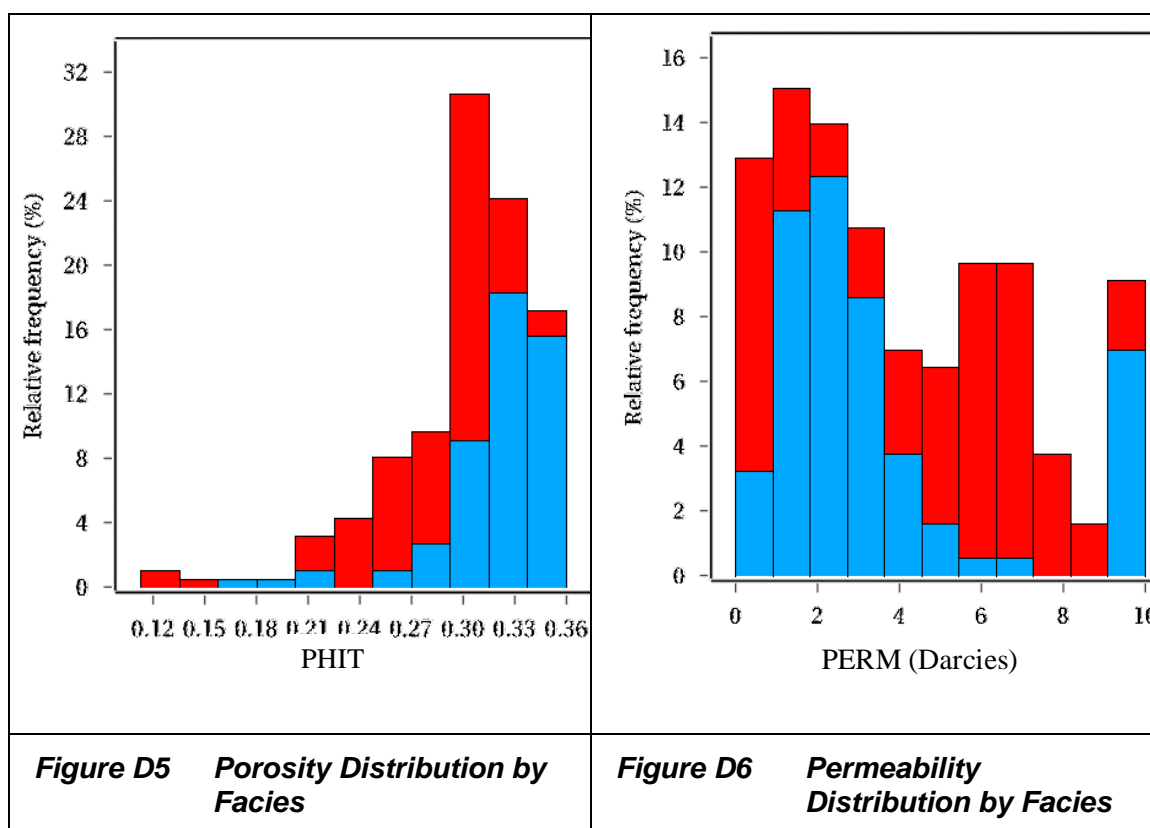


Figure D5: Porosity (PHIT) distribution in the wells (Sole-1 and Sole-2 combined) colour coded by facies (Braided Channels is red, Sheetflood is blue). There is no strong dependency between porosity and facies. The results of the facies modelling will therefore not have any significant impact on the porosity distribution as the porosity is similar, regardless of facies.

Figure D6: Permeability (PERM) distribution in the wells (Sole-1 and Sole-2 combined) colour coded by facies: The Braided Channels facies (red) has a more uniform spread of values (1-10 Darcies), while the permeability in the Sheetflood facies (blue) is concentrated around 1-3 Darcies. The permeability values are used to model Sw, so facies modelling was performed in the zones with variability of facies (main variability in LG_2 (subgrid 3), minor variability in LG_3 (subgrid 4)).

4.2 Facies Split in the Stratigraphic Units

The following facies split has been based on Sole-1 and Sole-2 :

- Subgrid 1 (Latrobe GP) 100 % Braided Channels
- Subgrid 2 (LG_1) 100 % Sheetflood
- Subgrid 3 (LG_2) 58% Sheetflood, 42% Braided Channels
- Subgrid 4 (LG_3) 5% Sheetflood, 95% Braided Channels
- Subgrid 5 (Top 20 m of Kate Shale E.) 100% Sheetflood

4.3 Investigation of Possible Trends in the Data

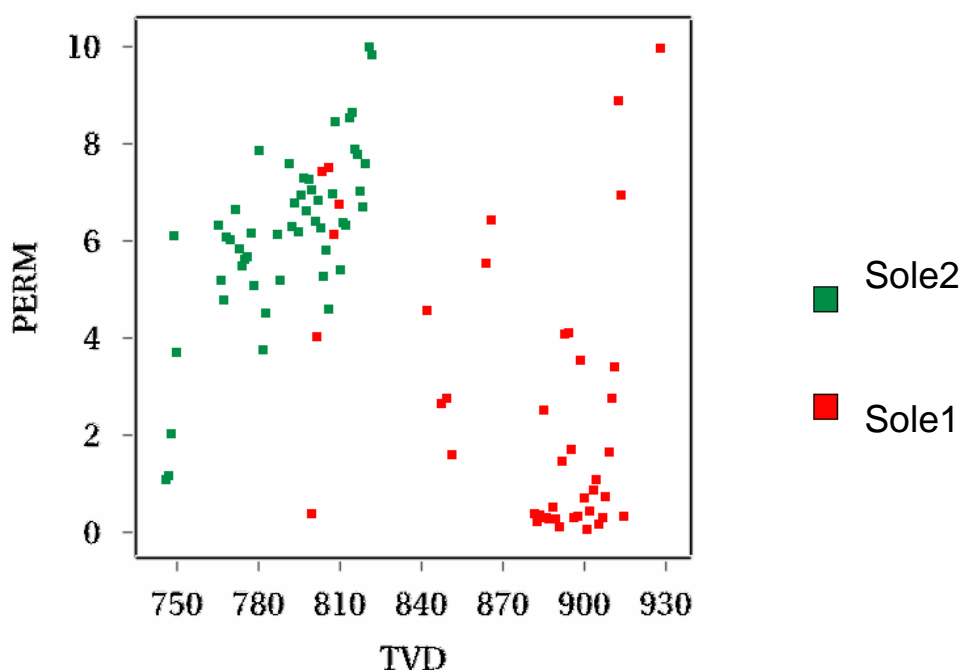
No trends were observed for porosity, but a trend for permeability (PERM) was observed in the Braided Channels facies (see Figure D7).

Sole-2 was drilled higher on the structure and further west than Sole-1. The permeability in the Braided Channels facies is higher in Sole-2 than Sole-1. The permeability in Sole-2 is mainly in the gas-zone, while Sole-1 is mainly in the water zone. There are several ways to interpret this:

- 1 A trend with depth.
- 2 A lateral trend (only two wells)
- 3 Different permeability transforms for the gas and the water zone.
- 4 Increased diagenetic effects in the aquifer compared to the gas reservoir.
- 5 A combination of the above.

It is assumed that 1) is the most likely explanation and has been used in the modelling.

Figure D7 Permeability (in Darcies) vs Depth in the Braided Channels Facies



Sole-2 has higher permeabilities in the Braided Channel facies than Sole-1. Sole-2 was drilled higher on the structure than Sole-1, so this may be interpreted to be a result of a general decreasing permeability with depth within this facies.

5 PROPERTY MODELLING

5.1 Facies

5.1.1 Base Case

The volume fractions of facies observed in the wells were used to populate the base case model. Facies modelling was performed only in Subgrid 3 (LG_2) and Subgrid 4 (LG_3). The other stratigraphic units (Latrobe GP, LG_1 and Top 20 m of the Kate Shale Equiv.) are homogeneous in the wells and assumed to contain only one facies type across the field:

- Subgrid 1 (Latrobe Gp) Braided Channels (single facies code)
- Subgrid 2 (LG_1) Sheetflood (single facies code)
- Subgrid 3 (LG_2) Braided Channels: size of objects around 3000*1000*5 m oriented EW (from dipmeter interpretation).
- Subgrid 4 (LG_3) Sheetflood (the 5% “remnant”): half the sizes of the above.
- Subgrid 5 (Top 20 m of Kate Shale Equivalent) Sheetflood (single facies code)

It should be noted that the sizes/orientation of the objects in Subgrid 3 and Subgrid 4 will not have any significant impact on GIP volumetrics. The porosity distribution is more or less facies independent. The water saturation is directly permeability derived (which is facies dependent), but the total facies split (volume fraction) is more or less the same, regardless of which shape/size the objects have.

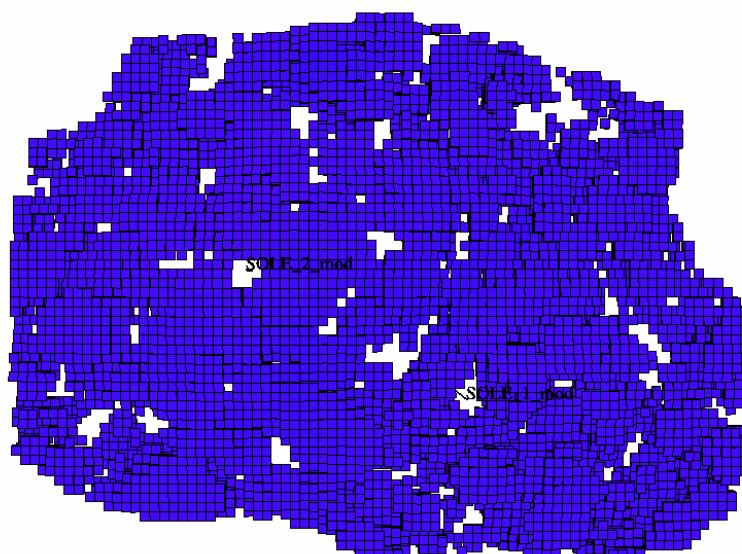
Ten stochastic realisations of facies distributions (in Subgrid 3 and Subgrid 4) have been generated and used as input for petrophysical modelling (see Section 5.2)

5.1.2 Conservative Scenario

The most significant aspect to GIP volumetrics, is a case where there are shales between the wells that are not seen in either Sole-1 or Sole-2.

If we model some shales randomly distributed between the wells, the shale volume cannot exceed 8% without dramatically increasing the chance of the two wells intersecting shale, which is not the case (Figure D8). Ten stochastic realizations of facies distributions with this conservative case have been generated and used as input for petrophysical modelling for the conservative case.

Figure D8 Model with 8% volume shale and all other facies filtered out



The figure shows shale bodies in plan view (approx. 8% of total volume). If we increase the amount of shale, the chance of neither well penetrating any shale (blue) is slim.

5.2 Porosity and Permeability

Transforms

The means and standard deviations have been estimated within each facies by each subgrid. The depth trend in the Braided Channel facies (decreasing permeability by depth, see Figure D7) was included in the modelling.

Variogram Ranges

Vertical direction: 10 m in the vertical direction was estimated from the well logs.

Lateral directions: 3000*1000m was used as the lateral range, where the longest axis of the variogram (3000m) was oriented parallel to the general depositional direction estimated from dipmeter.

Correlations

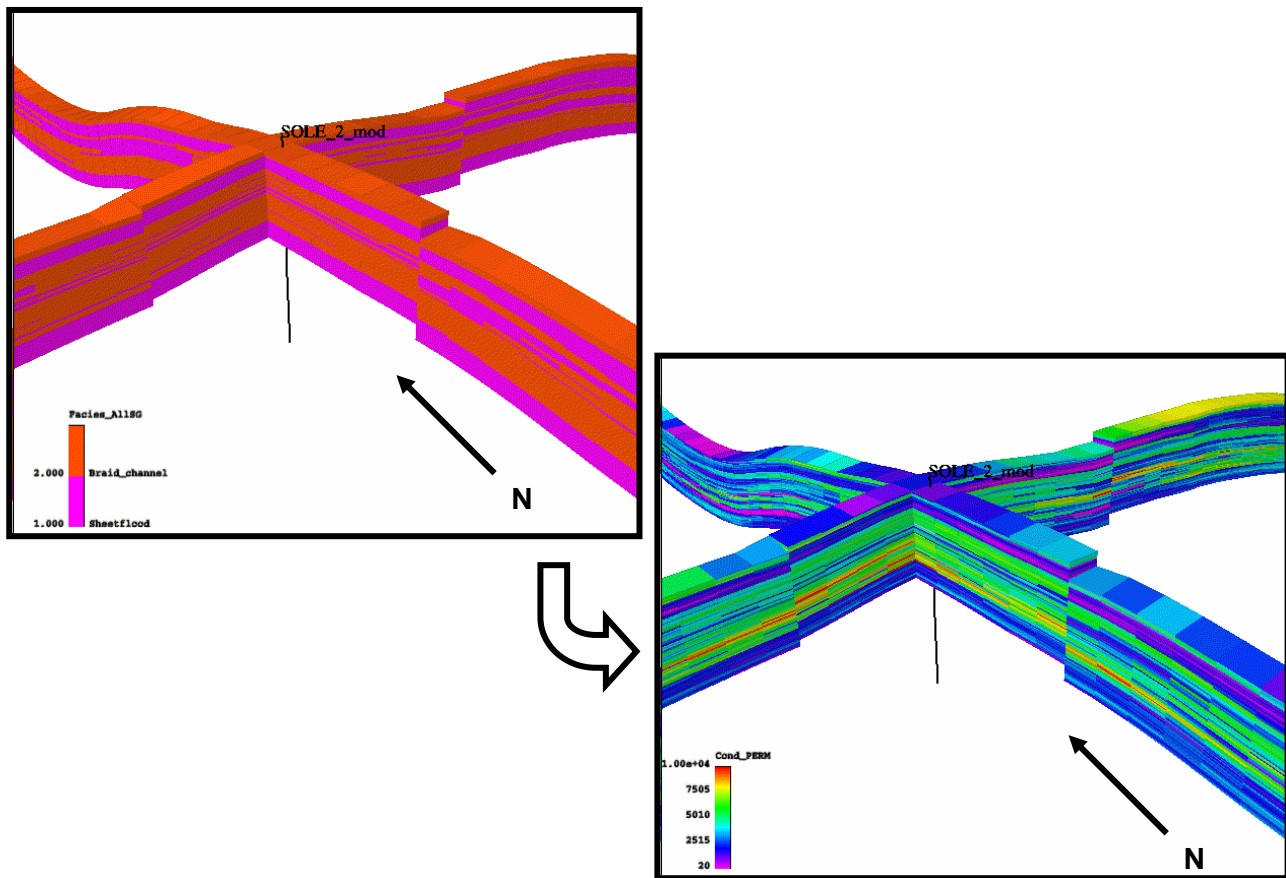
The Porosity-Permeability correlation factors were estimated from the well logs:

- Sheetflood facies 0.47
- Braided channel facies 0.78

Product

Ten realisations of petrophysics conditioned to facies for both scenarios (base case and conservative case) were generated. One example for one realisation of the base case scenario is shown in Figure D9.

Figure D9 **Petrophysical Conditioning**



One realisation of facies results in a corresponding realisation of permeability. Wherever the facies code has been set to Braided Channel (orange in the facies parameter), the permeability in the same location for the same realization is concentrated around 1-3 Darcies (bluish in the permeability parameter).

5.3 Water Saturation

The water saturation modelling is based on the following function (ref. Part B, Petrophysics)

$$S_w = a \cdot (h - h_d)^{-\lambda}$$

where for Sheetflood (high GR): $a = -0.489 \cdot \log(K_{is}) + 1.916$

$$\lambda = -0.040 \cdot \log(K_{is}) + 0.39$$

$$h_d = 0.420 \cdot \log(K_{is}) - 0.939$$

and for Braided Channels (low GR): $a = -0.174 \cdot \log(K_{is}) + 0.996$

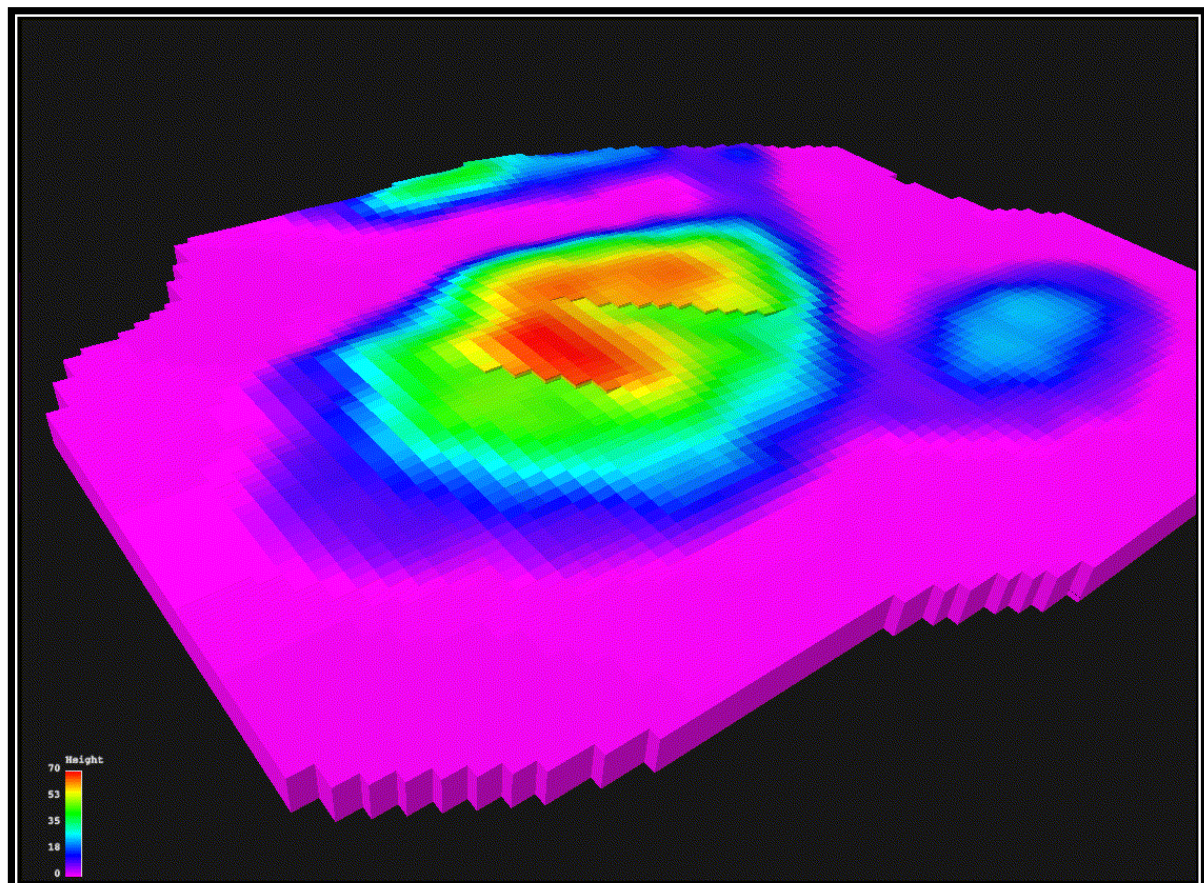
$$\lambda = 0.087 \cdot \log(K_{is}) + 0.003$$

$$h_d = 0.039 \cdot \log(K_{is}) + 0.082$$

where K_{is} is the in-situ permeability expressed in milliDarcies, h is the height above the FWL in metres (See Figure D10) and S_w is the water saturation expressed as a fraction of pore volume.

This formula was implemented in a script stored within the RMS project. The script reads all necessary information (facies code, permeability and height above the FWL), and outputs a 3D distribution of water saturation. The script was run for every realisation, to ensure consistency between the water saturation and the facies and permeability distribution. The water saturation was set to 40% for the cells where the height is less than 1 meter.

Figure D10 ***Height above Free Water Level used in the Water Saturation Calculations***



The maximum height is around 70 meters (red) at the crest.

6 VOLUMETRICS (GIP)

The volumes (GIP) have been calculated based on 10 realisations of properties for four different scenarios. These scenarios are described in Sections 6.1-6.4. Common for all scenarios are

- GWC = 816.5 m
- Bg = 0.012
- Net/Gross = 1 (In the scenario described in Section 6.2, the porosity is set to 0 in the shales).

6.1 Base Case GIP

By using the most likely structural map and facies volume fractions, the variation in GIP is shown in Table D1. The mean is close to the GIP in Realisation 8, so this realisation is used as the most representative for the base case when upscaling and exporting to Eclipse.

The GRV is 496.0 MMm³.

Table D1 Base Case GIP

Real #	GIP (BCF)	Rank
1	367.4	1
2	358.0	8
3	347.4	10
4	348.9	9 (P90)
5	358.3	7
6	361.1	4
7	366.7	2 (P10)
8	358.5	6
9	361.2	3
10	359.4	5
<i>Mean</i>	<i>358.7</i>	

6.2 GIP Effect of 8% shales Between the Wells

By using the most likely structural map and with 8% shale facies between the wells (i.e. a conservative case), the variation in GIP is shown in Table D2.

The GRV is the same as in the base case (496.0 MMm³)

Table D2 **GIP Effect of 8% Shales Between the Wells**

Real #	GIP (BCF)	GIP in Base c.	%
1	332.9	367.4	-9.4
2	320.9	358.0	-7.6
3	319.8	347.4	-7.9
4	318.3	348.9	-8.8
5	323.6	358.3	-9.7
6	335.9	361.1	-7.0
7	337.9	366.7	-7.9
8	325.4	358.5	-9.2
9	326.4	361.2	-9.6
10	330.4	359.4	-8.1
Mean	327.2		-8.8

6.3 GIP Effect of Optimistic Seismic Pick

No significant structural uncertainty is assumed in the centre of the field, where both the GWC and Top Latrobe are clearly separated. However, uncertainty is recognized at the reservoir limits, where the GWC and Top Latrobe picks interfere, namely where the gas column is less than 8-10 m. An alternative seismic depth map of Top Latrobe, which outlines the maximum reasonable extent of Top Latrobe above the GWC was created (Ref Part C).

To calculate the GIP for the structural upside, the most likely map of Top Latrobe was replaced with this optimistic map of Top Latrobe. Stratigraphic modelling was then rerun and parameters resampled before GRV, water saturation and the resulting GIP were recalculated. The results are shown in Table D3.

The GRV is 538.5 MMm³ (8.6% higher than base case). The difference in % (+8.6% GRV results in only +5.8% GIP) is reasonable as a result of the addition of GRV with higher associated Sw due to its location along the flanks.

Table D3 **GIP Effect of Optimistic Seismic Pick**

Real #	GIP (BCF)	GIP in Geomodel	%
1	389.8	367.4	6.1
2	380.7	358.0	6.3
3	366.9	347.4	5.6
4	368.1	348.9	5.7
5	377.5	358.3	5.4
6	383.4	361.1	6.2
7	388.1	366.7	6.2
8	378.8	358.5	5.7
9	382.3	361.2	5.8
10	379.7	359.4	5.6
Mean	379.5	358.7	5.8

6.4 GIP Effect of Conservative Seismic Pick

A polygon was created to define the minimum reasonable extent of Top Latrobe above the GWC (where the GWC and Top Latrobe interfere, i.e where the gas column is less than 8 –10 meters thick) - Ref Part C.

The GIP for the structural downside was calculated by eliminating all cells of the base model outside this polygon. The results are shown in Table D4.

The GRV is 482.1 MMm³ (2.8% lower than the base case). The percentage difference (-2.8% GRV results in only -1.8% GIP) is reasonable as this case represents the removal of GRV with higher associated Sw where the reservoir is thin along the outer flanks.

Table D4 GIP Effect of Conservative Seismic Pick

Real #	GIP (BCF)	GIP in Geomodel	%
1	360.7	367.4	-1.8
2	350.9	358.0	-2.0
3	341.4	347.4	-1.7
4	342.8	348.9	-1.7
5	352.0	358.3	-1.8
6	353.7	361.1	-2.0
7	359.8	366.7	-1.9
8	352.2	358.5	-1.8
9	354.6	361.2	-1.8
10	352.9	359.4	-1.8
Mean	352.1	358.5	-1.8

6.5 Summary of GIP Volumetrics from 3D modelling

- The “base case” has a GIP of 358.5 BCF gas.
- There is some uncertainty related to seismic pick along the edge of the reservoir. The upside may increase the GIP to around 380 BCF. The corresponding downside may reduce the GIP to around 350 BCF.
- There is a speculative downside related to possible shale objects between the wells. This may decrease the GIP to around 320 BCF.
- The impact on GIP due to the uncertainty of the parameter distribution (reservoir facies, porosity and water saturation) in each of these scenarios is small (approx. \pm 3%).

In addition to this, there are two speculative downside scenarios:

1. A downside scenario could arise from a regional facies boundary somewhere in the field that is not observed on seismic or in the two wells. This could decrease the reserves significantly, but there is nothing in the wells or seismic data that indicates the likelihood of such a scenario.
2. Another downside could be if there are facies (shales or coals) in the northeastern part of the field (in the saddle separating the northern and central lobes part of the field, see Figure D1). This could prevent communication between these lobes. The volumes in this northern lobe of the field (north of the saddle to the northeast) constitute 10.4% of the total GRV and 10.0% of the total GIP in the Sole field. The likelihood of such facies development in the critical area is again considered low.

Figure D11 *GIP in modelled scenarios*

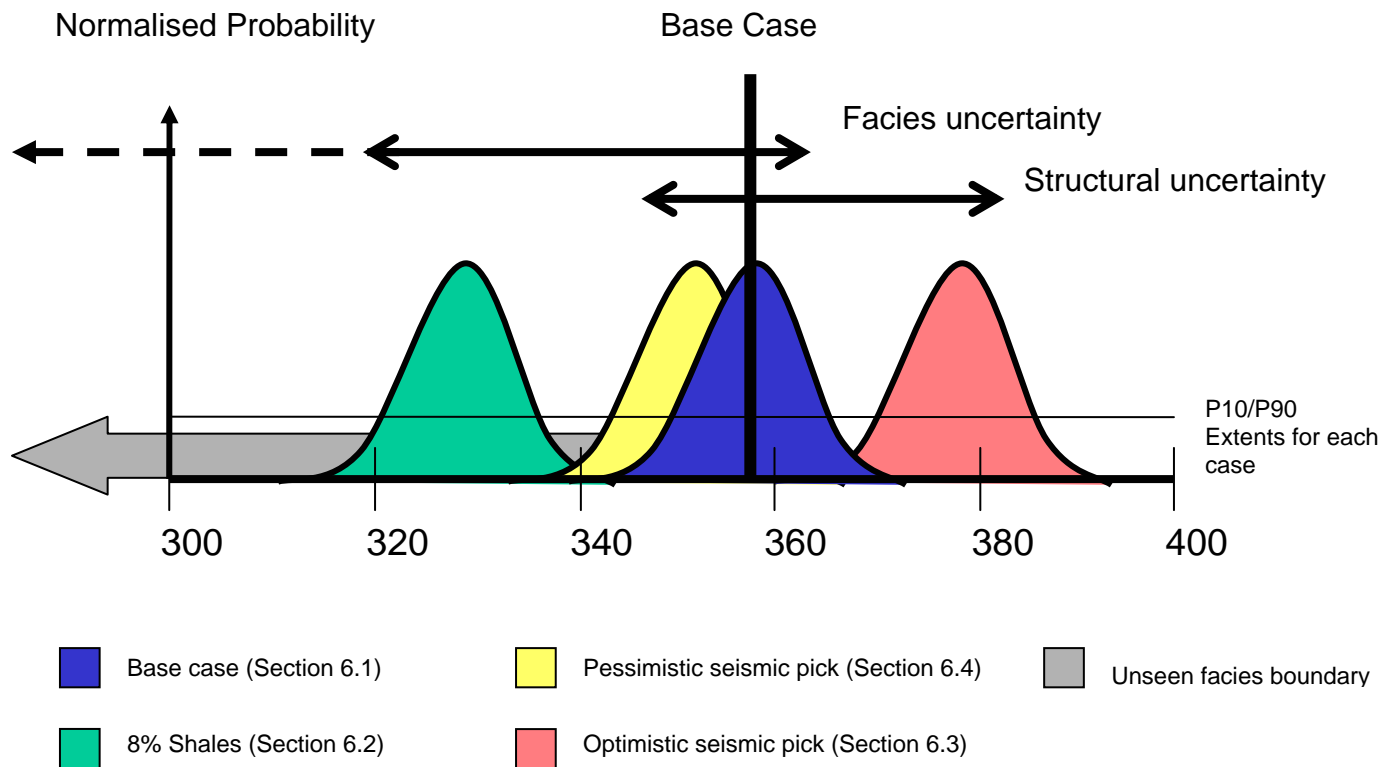


Figure D11 illustrates the effect on GIP of different seismic picks and distribution of shales between the wells.

7 SIMULATION GRID DESIGN

A simulation grid was generated with approximately a 2*2*2 coarsening of the geological model:

- | | |
|---|----------------------------|
| • Subgrid 1 (Latrobe GP) | 3 layers (6 in geomodel) |
| • Subgrid 2 (LG_1) | 6 layers (12 in geomodel) |
| • Subgrid 3 (LG_2) | 12 layers (25 in geomodel) |
| • Subgrid 4 (LG_3) | 15 layers (30 in geomodel) |
| • Subgrid 5 (Top 20m of Kate Shale Eq.) | 10 layers (20 in geomodel) |

The XY resolution was set to 40*30 cells (approximately 200*200m), resulting in a total number of 55,200 cells. No Local Grid Refinements or varying grid resolution was required.

The GRV in the RMS simulation grid is 494.5 MMm³ (vs 496.0 in geomodel).

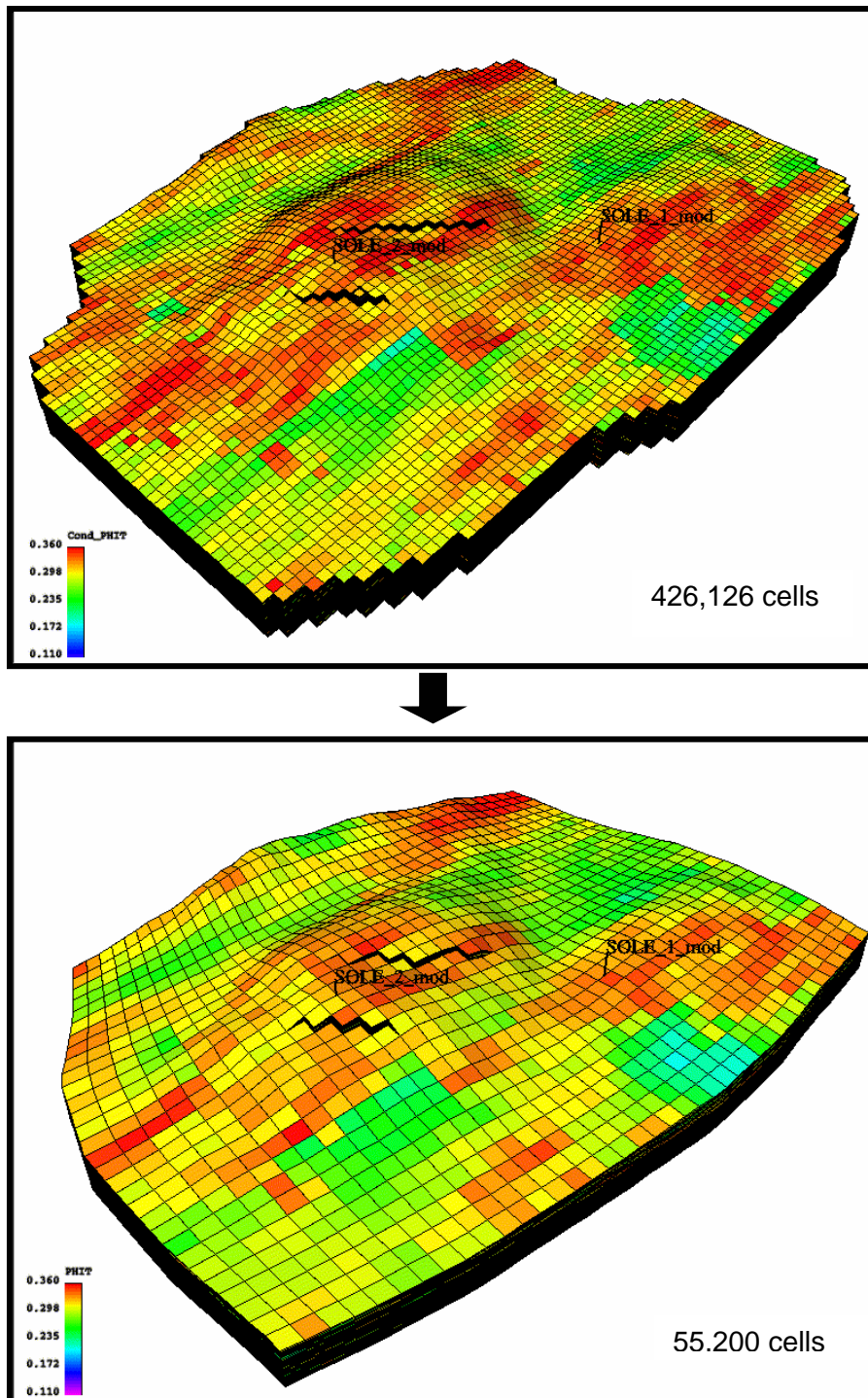
Volume factor Simgrid>geomodel: 1.00316 (0.3 % difference).

8 UPSCALING AND GRID EXPORT FOR SIMULATION

The following upscaling methods were used:

- Porosity and water saturation: Arithmetic averaging, weighted by GRV.
- Permeability in X and Y direction: Diagonal tensor, using modelled permeability as input.
- Permeability in Z direction (vertical permeability): Diagonal tensor, using modelled permeability*0.75 as input. (This was done to take into account the Kv/Kh relationship of 0.75 measured from core).

Figure D12 *Illustration of the Upscaling Process of Porosity*



The GIP in the simulation grid was then calculated for all the realizations of the base case scenario. The results are shown in Table D5:

Table D5 Comparison Simulation Model vs Geological Model Volumetrics

Real #	GIP (BCF)	GIP in Geomodel	Rank
1	366.8	367.4	1
2	357.3	358.0	8
3	346.5	347.4	10
4	348.1	348.9	9 (P90)
5	356.9	358.3	7
6	360.4	361.1	4
7	366.1	366.7	2 (P90)
8	357.7	358.5	6
9	360.4	361.2	3
10	358.6	359.4	5

The simulation grid for the four main scenarios were exported to Eclipse with the parameters PORO, PERMX, PERMY and PERMZ.

The units were converted to Field units (Ft³*Ft³*Ft) during export.